Distribution System State Estimation Using an Artificial Neural Network Approach for Pseudo Measurement Modeling

Efthymios Manitsas, *Member, IEEE*, Ravindra Singh, *Member, IEEE*, Bikash C. Pal, *Senior Member, IEEE*, and Goran Strbac, *Member, IEEE*

***Abstract*—This paper presents an alternative approach to pseudo measurement modeling in the context of distribution system state estimation (DSSE). In the proposed approach, pseudo measurements are generated from a few real measurements using artificial neural networks (ANNs) in conjunction with typical load profiles. The error associated with the generated pseudo measurements is made suitable for use in the weighted least squares (WLS) state estimation by decomposition into several components through the Gaussian mixture model (GMM). The effect of ANN-based pseudo measurement modeling on the quality of state estimation is demonstrated on a 95-bus section of the U.K. generic distribution system (UKGDS) model.**

***Index Terms*—Artificial neural networks, distribution system state estimation, Gaussian mixture model, pseudo measurement modeling.**

NOMENCLATURE

e_i	ANN error in the ith time step.
e_V, e_δ	Average relative errors in voltage magnitude and voltage angle estimates, respectively.
$\mathbf{e_z}$	Measurement error vector.
$f(j\|e_i,\gamma)$	Marginal probability density of the jth mixture component.
$\boldsymbol{G}$	System gain matrix.
$\boldsymbol{H}$	System Jacobian matrix.
$\mathbf{h}(\mathbf{x})$	Nonlinear function of measurements.
m	Number of measurements.
M_c	Number of Gaussian mixture components.
n	Number of state variables.
$\hat{\boldsymbol{P}}_x$	Estimated state error covariance matrix.
$\boldsymbol{R}_z$	Measurement error covariance matrix.
$\hat{S}_{flow}$	Estimated line power flow.
$S_{\max}$	Line rating.
$\hat{V}^i$, $\hat{\delta}^i$	Estimated value of voltage magnitude and voltage angle at the ith bus, respectively.
V_t^i, δ_t^i	True value of voltage magnitude and voltage angle at the ith bus, respectively.
w_i, μ_i, σ_i^2	Weight, mean, and variance of the ith Gaussian mixture component, respectively.
$\hat{\mathbf{x}}$	Estimated state vector.
$\mathbf{z}$	Measurement vector.
γ	Set of parameters of mixture components.
σ_g	Standard deviation of secondary variable.
σ_{zi}	Standard deviation of the ith measurement.
$\mathcal{N}$	Gaussian probability density function.

Manuscript received June 16, 2011; revised September 02, 2011 and December 12, 2011; accepted February 06, 2012. Date of publication April 03, 2012; date of current version October 17, 2012. Paper no. TPWRS-00571-2011.

The authors are with the Department of Electrical and Electronic Engineering, Imperial College London, London, U.K. (e-mail: e.manitsas06@ic.ac.uk; ravindra.singh@ic.ac.uk; bcpal@ieee.org; g.strbac@ic.ac.uk).

Color versions of one or more of the figures in this paper are available online at http://ieeexplore.ieee.org.

Digital Object Identifier 10.1109/TPWRS.2012.2187804

I. INTRODUCTION

THE bulk of the power distribution system infrastructure in developed countries was built in the 1950s and 1960s. Distribution systems were designed and built to accommodate the expected seasonal demand variations and projected demand growth and were operated passively, without monitoring and control. They were the unidirectional links between the transmission system and the individual demand.

In the last decade, there is a paradigm shift in the approach of stakeholders on the way distribution systems should be operated. This development is mainly driven by new regulatory frameworks and incentives towards the integration of distributed generation (DG) in distribution systems and accommodation of demand side participation in the control of system voltage and frequency. In this context, it is widely accepted that active management (AM) is the most effective approach to distribution system operation [1].

To enable AM in distribution systems, a distribution management system (DMS) with its corresponding telecommunication, monitoring, computation, and control functions is required. Government directives towards the introduction of smart metering to all consumers intend to alleviate the lack of monitoring in current distribution systems. However, it is not yet clear how the associated communication infrastructure will evolve in order to transmit the envisaged volume of measurements to the DMS. Furthermore, the smart metering infrastructure will be primarily used to record energy information which will be communicated to the DMS irregularly. On the other hand, the state estimation function requires power injection measurements at regular intervals. In view of these, it is necessary to introduce computational techniques that compensate the lack

of monitoring in distribution systems and improve the accuracy of the state estimation function.

While state estimation is a fairly routine task in transmission systems and a host of state estimation techniques exist, these cannot be simply migrated to distribution systems mainly due to lack of available measurements and lack of methodologies and tools that can be applied to limited measurements.

Research on distribution system state estimation (DSSE) methodologies started appearing in the literature in the 1990s. Roytelman and Shahidehpour presented a DSSE technique taking into consideration the small number of measurements in the distribution system [2]. Baran and Kelley introduced state estimation in distribution networks in order to improve forecasted load data using real time measurements [3] while Lu, Teng, and Liu proposed a current-based DSSE technique [4]. Likewise, a current-based three-phase fast decoupled state estimation method with measurement pairing is discussed in [5]. State estimation using an artificial neural network (ANN) is presented in [6]. In this approach, an ANN is used to directly estimate both voltage magnitudes and power injections using the voltage magnitude at the main substation and a relatively large number of real injection measurements.

The DSSE function is presented with the formidable task of providing reasonable and meaningful estimates of the system states using very limited measurements. First of all, this is not feasible unless pseudo measurements are introduced in order to ensure the observability of the system. Furthermore, pseudo measurements need to be accurately modeled so that the quality of the estimates is improved.

Load values obtained from load profiles have been typically used as pseudo measurements. These load values are, in effect, high variance estimates of the customer load behavior. Consequently, the quality of the state estimates obtained with this approach is generally poor. Furthermore, the values obtained with the use of load profiles may not be synchronized with the substation and DG measurements at a given point in time, introducing further inaccuracy.

Pseudo measurements, missing measurements, and load modeling issues have been addressed by a number of researchers. The use of a probabilistic associative memory to deal with missing measurements is proposed in [7]. A fuzzy load allocation technique for use in a DMS environment is described in [8] while load correlation is introduced in the load allocation routine in [9]. The authors in [10] present two approaches to modeling of pseudo measurement, one based on correlation and one based on load probability density functions. A probabilistic neural network approach for assigning load profiles to consumers is proposed in [11]. In [12] ANNs are used to solve data acquisition and processing problems, with training data obtained either from load flow or the supervisory control and data acquisition (SCADA) system. A pseudo measurement modeling approach based on the Gaussian mixture model (GMM) is presented in [13].

An efficient way to model load pseudo measurements is to express them as nonlinear functions of measurements available at main substations and/or DG locations. In a small system, this function can be easily obtained explicitly by solving a curve fitting problem. However, obtaining this function in large systems is a challenging task. This was the motivation in using ANNs with their inherent capability to infer a function from observations.

In this paper, an ANN approach for modeling active and reactive power injection pseudo measurements in DSSE is presented. Load profiles and a small number of power flow measurements derived from load flow simulations are used to train ANNs. The error between the target power injections and the output of the ANNs is modeled through the GMM. During DSSE execution real measurements are used as input to the ANNs in order to produce the pseudo measurements. The error model is used to generate the variance of the pseudo measurements.

Following this introduction, a brief description of state estimation is presented in Section II while the mathematical model of ANNs is introduced in Section III. The proposed methodology is described in Section IV. The simulation study is detailed in Section V, and results and discussions are presented in Section VI.

II. State Estimation

The widely used weighted least squares (WLS) algorithm is employed for estimating the state of the distribution system under the "normal measurements" assumption [14]. WLS [15] is based on minimization of the following objective:

$$J' = [\mathbf{z} - \mathbf{h}(\mathbf{x})]^T \boldsymbol{R}_z^{-1} [\mathbf{z} - \mathbf{h}(\mathbf{x})] \tag{1}$$

where $\mathbf{z}$ and $\mathbf{x}$ are the vectors of measurements and state components, respectively. It is assumed that these vectors are related according to the equation $\mathbf{z} = \mathbf{h}(\mathbf{x}) + \mathbf{e}_z$, where $\mathbf{h}(\mathbf{x})$ is a known function. The measurement error vector $\mathbf{e}_z \sim \mathcal{N}(\mathbf{0}, \boldsymbol{R}_z)$ is assumed to be a Gaussian random variable with covariance matrix $\boldsymbol{R}_z = \mathrm{diag}\{\sigma_{z1}^2, \sigma_{z2}^2, \ldots, \sigma_{zm}^2\}$, i.e., cross correlation between metering errors [16] is not taken into consideration. Thus, σ_{zi}^2 is the variance of the ith measurement.

The minimizer $\hat{\mathbf{x}}$ for the WLS objective is obtained as the limit of a sequence of states $\{\hat{\mathbf{x}}_k\}$ by means of a recursive scheme, one step of which is

$$\hat{\mathbf{x}}_{k+1} = \hat{\mathbf{x}}_k + \boldsymbol{G}(\hat{\mathbf{x}}_k)^{-1} \boldsymbol{H}^T(\hat{\mathbf{x}}_k) \boldsymbol{R}_z^{-1} [\mathbf{z} - \mathbf{h}(\hat{\mathbf{x}}_k)] \tag{2}$$

where

$$\boldsymbol{H}(\hat{\mathbf{x}}_k) = \left[\frac{\partial \mathbf{h}(\mathbf{x})}{\partial \mathbf{x}} \right]_{\mathbf{x} = \hat{\mathbf{x}}_k} \tag{3}$$

$$\boldsymbol{G}(\hat{\mathbf{x}}_k) = \boldsymbol{H}^T(\hat{\mathbf{x}}_k) \boldsymbol{R}_z^{-1} \boldsymbol{H}(\hat{\mathbf{x}}_k). \tag{4}$$

$\boldsymbol{H}$ and $\boldsymbol{G}$ are the system Jacobian and Gain matrices, respectively.

The state vector $\hat{\mathbf{x}} = [\hat{V}^1 \ldots \hat{V}^n \ \hat{\delta}^2 \ldots \hat{\delta}^n]^T$ in which $\hat{V}^i$, $\hat{\delta}^i$ are the estimated values of voltage magnitude and voltage angle at the ith bus, respectively, and n is the number of buses. Bus 1 is the reference bus with $\hat{\delta}^1 = 0$.

An estimate of the state error covariance matrix $\hat{\boldsymbol{P}}_x$ at $\hat{\mathbf{x}}$ is given by [17]

$$\hat{\boldsymbol{P}}_x = [\boldsymbol{G}(\hat{\mathbf{x}})]^{-1}. \tag{5}$$

The state estimates $(\hat{\mathbf{x}})$, the bus voltage magnitudes and angles, are known as primary variables because they are directly

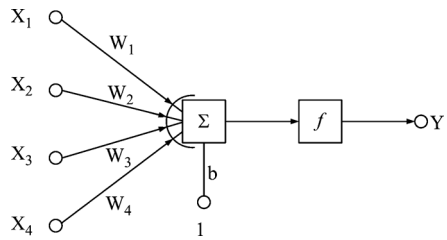

Fig. 1. Neuron.

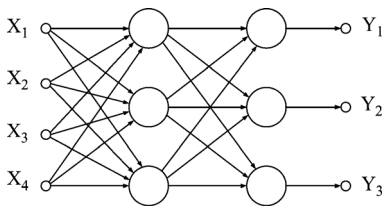

Fig. 2. Two-layer feed-forward ANN.

obtained from the state estimation algorithm. The diagonal elements of $\hat{\boldsymbol{P}}_x$ represent the variance of the estimation errors associated with the primary variables. The estimates of other variables such as line power flows, line currents, and bus power injections are derived from the primary variables using their functional relationships. These variables are called the secondary variables. The accuracy of the secondary variables is determined by the accuracy of the primary variables and, hence, if the state estimation error covariance matrix $\hat{\boldsymbol{P}}_x$ is known, the variance of a secondary variable can be computed as follows:

$$\sigma_g^2 = \left[\frac{\partial g(\mathbf{x})}{\partial \mathbf{x}}\right]_{\mathbf{x}=\hat{\mathbf{x}}} \hat{\boldsymbol{P}}_x \left[\frac{\partial g(\mathbf{x})}{\partial \mathbf{x}}\right]^T_{\mathbf{x}=\hat{\mathbf{x}}} \tag{6}$$

where $g(\mathbf{x})$ is the functional expression of a secondary variable.

III. Artificial Neural Networks

An ANN is a mathematical model that is based on the architecture and functionality of biological neural networks [18], [19]. The most common use of ANNs is regression analysis, classification, and data processing.

The elemental building unit of an ANN is the neuron. The neuron receives a number of inputs X, processes them, and generates a response Y. First, the inputs X are linearly combined using the weights w_i and a constant bias b. The result is then used as the argument of the transfer function f. The transfer function f is differentiable and non-decreasing. Typical transfer functions are the sigmoid and the linear. A neuron with four inputs is shown in Fig. 1.

In this paper, two-layer feed-forward ANNs are used. As shown in Fig. 2, the neurons are organized in two layers, one hidden, i.e., between the input nodes and the output layer, and the output layer. The ANN is designated as feed-forward as the outputs of one layer are the inputs to the next layer. The hidden layer uses sigmoid transfer functions and the output layer linear ones.

The ANN parameters are estimated (the ANN is trained) by minimizing a loss function. In this work, the scaled conjugate gradient back propagation optimization method is used. This method exhibits linear/superlinear convergence and is suitable for large scale problems [20].

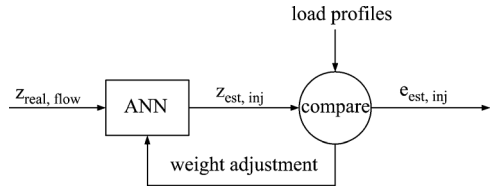

Fig. 3. ANN training.

IV. Proposed Methodology

The proposed approach comprises three stages: the ANN training stage, the error modeling stage, and the state estimation application stage.

A. ANN Training

At first, two ANNs are trained so that particular sets of real power flow measurement inputs lead to specific sets of power injection outputs. The first ANN associates real active power flow measurements with active power injections, and the second ANN relates real reactive power flow measurements with reactive power injections. Each ANN is adjusted by comparing its output with the target load profiles. Attention is given so that no over fitting takes place, i.e., the ANN can generalize so that there are no large errors when new real power flow measurements are used as input.

The ANN training concept is shown in Fig. 3. Real power flows are used as inputs. The output of the ANN, which is the estimate of the power injections, is compared with the load values coming from the load profiles at the specific time step. The ANN weights are adjusted and the procedure is repeated with the next set of real power flows and loads.

To summarize, the ANN training procedure involves the following steps:

Step 1) Use mix of consumer classes for each bus and synthesize load profiles for the whole year.

Step 2) Run load flow simulation for the whole year using load profiles and save selected active and reactive power flows.

Step 3) Train ANNs using selected active and reactive power flows as input and load profiles as target output.

Step 4) Save error between ANN target output (load profiles) and ANN output for further processing.

Alternatively, the same ANNs can be trained using any set of random loads obtained through Monte Carlo simulations provided that the resulting load flow converges.

The ANN configuration, training, and testing were performed using MATLAB [21].

B. Error Modeling

The probability density of a typical ANN output error (difference between load profiles and ANN power injection outputs) is shown in Fig. 4. It is obvious from the figure that the ANN error does not follow the Gaussian distribution. It has been shown in

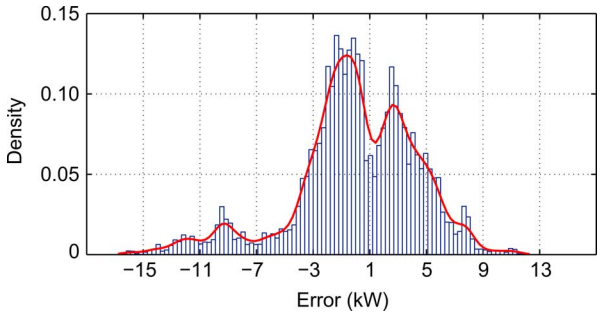

Fig. 4. Probability density of typical ANN error.

[14] that the consistency of the WLS state estimation relies on the assumption that measurements are normally distributed. In this work, the ANN error is processed using the GMM algorithm.

A GMM is the weighted finite sum of several Gaussian components. A multivariate GMM is characterized by a set of weights, mean vectors, and covariance matrices of the mixture components and mathematically can be expressed as

$$f(e|\gamma) = \sum_{i=1}^{M_c} w_i f\left(e|\mu_i, \sigma_i^2\right) \tag{7}$$

where M_c is the number of mixture components and w_i is the weight of the ith mixture component, subject to $w_i > 0$ and $\sum_{i=1}^{M_c} w_i = 1$. γ is chosen from the set of parameters $\Gamma = \{\gamma : \gamma = \{w_i, \mu_i, \sigma_i^2\}_{i=1}^{M_c}\}$, each member of which defines a Gaussian mixture. The density function of each mixture component $f(e|\mu_i, \sigma_i^2)$ is a normal distribution.

Details on the GMM formulation for load modeling in distribution systems can be found in [22].

In the proposed methodology, the error in each power injection estimate is modeled through a set of M_c mixture components. Then, each error is associated with a specific mixture component and the resulting variance is saved along with the corresponding error timestamp.

1) Error Association: An error is associated with the jth Gaussian component in the mixture through data association using the relative marginal density given by

$$f(j|e_i, \gamma) = \frac{w_j f(e_i|\mu_j, \sigma_j^2)}{\sum_{k=1}^{M_c} w_k f(e_i|\mu_k, \sigma_k^2)} = \frac{w_j \mathcal{N}\left(\mu_j, \sigma_j^2\right)(e)}{\sum_{k=1}^{M_c} w_k \mathcal{N}\left(\mu_k, \sigma_k^2\right)(e)}. \tag{8}$$

Using (8), the relative marginal density of the error at a specific time step with respect to each component is computed. The component with the maximum density is identified as representative of the error. If several components have comparable marginal densities, they can be merged together using the mixture reduction technique described in [13].

The error modeling concept is demonstrated in Fig. 5.

C. State Estimation Application

In the context of state estimation, the previously described ANN and error models are used to create the required power injection pseudo measurements. The execution of state estimation involves the following steps:

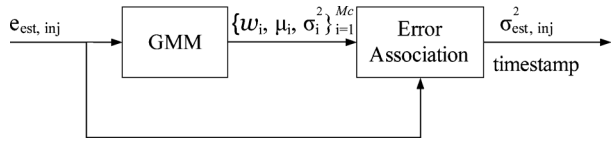

Fig. 5. Error modeling.

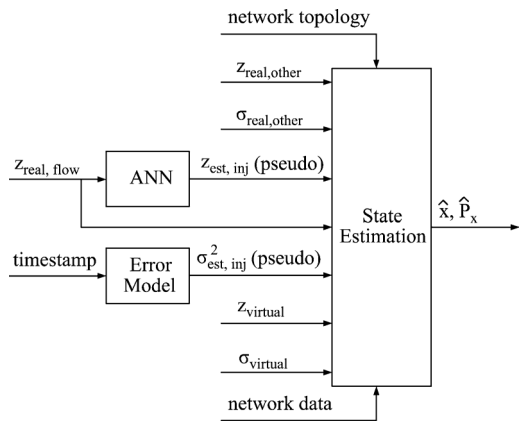

Fig. 6. State estimation application.

Step 1) At time t, use the real active and reactive power flow measurements as input to the ANNs.

Step 2) Obtain the active and reactive power injections at time t from the output of the ANNs and store them as pseudo measurements.

Step 3) Compare the output of ANN with the load values obtained from the load profiles and compute the error in pseudo measurements at time t.

Step 4) Associate the error computed in Step 3 with a GMM component in the error model and obtain the variance of active and reactive power injection pseudo measurements corresponding to this error.

Step 5) Use real and pseudo measurements along with their variances to construct the $\boldsymbol{R}_z$ matrix in (1) for state estimation.

Step 6) Repeat Steps 1 to 6 for other time steps.

Overall, the inputs to the state estimation function are real measurements (voltage magnitudes, active and reactive power flows, and active and reactive power injections), pseudo measurements (active and reactive power injections), virtual measurements (zero injection buses), and the network topology and parameters. All measurements are used with their corresponding standard deviations.

The state estimation execution concept is shown in Fig. 6.

V. Simulation Study

The performance of the proposed methodology was tested on a part of the U.K. Generic Distribution System (UKGDS) model. The 11-kV system considered comprises 95 buses, 94 lines, 54 loads and two DGs, as shown in Fig. 7. The system parameters and load information for the UKGDS were obtained from [23]. The buses were renumbered for convenience.

The UKGDS assumes four classes of consumers: Domestic-Unrestricted (D/U), Domestic-Economy (D/E), Industrial (I), and Commercial (C). Half hourly normalized active power load

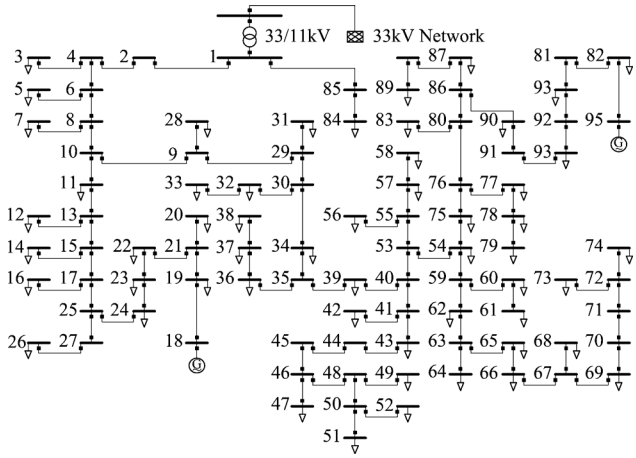

Fig. 7. Test network.

TABLE I
SUMMARY OF SCENARIOS

Scenario	ANN Input	Real Measurements
1	P_{1-2}, Q_{1-2}	V_1 $P_{1-2}, Q_{1-2}, P_{1-85}, Q_{1-85}$ $P_{18}, Q_{18}, P_{84}, Q_{84}, P_{95}, Q_{95}$
2	P_{1-2}, Q_{1-2} P_{15-17}, Q_{15-17} P_{34-35}, Q_{34-35}	V_1 $P_{1-2}, Q_{1-2}, P_{1-85}, Q_{1-85}$ $P_{15-17}, Q_{15-17}, P_{34-35}, Q_{34-35}$ $P_{18}, Q_{18}, P_{84}, Q_{84}, P_{95}, Q_{95}$
3	P_{1-2}, Q_{1-2} P_{15-17}, Q_{15-17} P_{34-35}, Q_{34-35}	$V_1, V_{19}, V_{20}, V_{21}$ $P_{1-2}, Q_{1-2}, P_{1-85}, Q_{1-85}$ $P_{15-17}, Q_{15-17}, P_{34-35}, Q_{34-35}$ $P_{18}, Q_{18}, P_{84}, Q_{84}, P_{95}, Q_{95}$

profiles over one year along with their annual maximum demand are provided for each consumer class. The methodology followed to obtain the load profiles from the mix of consumer classes at each bus is given in [23].

The three scenarios examined are presented in Table I. Voltage magnitudes and voltages angles are selected as the state variables in state estimation. Bus 1 is considered to be the reference bus with voltage angle equal to zero.

Two ANN variations for pseudo measurement modeling are considered. The first variation is based on the assumption that a single set of real power flow measurements is available at the substation (P_{1-2}, Q_{1-2}). The second variation uses two additional sets of power flow measurements (P_{15-17}, Q_{15-17} and P_{34-35}, Q_{34-35}), in accordance with the optimal measurement placement algorithm presented in [24].

Real measurements are assumed to be mainly available at the substation and the DG locations. Thus, the voltage magnitude at bus 1 (V_1), the active and reactive power flows in lines 1–2 and 1–85 (P_{1-2}, Q_{1-2} and P_{1-85}, Q_{1-85}), the active and reactive power injections at bus 18 and bus 95 (P_{18}, Q_{18} and P_{95}, Q_{95}) and, for completion, the active and reactive power injections at bus 84 (P_{84}, Q_{84}) were considered as real measurements in Scenario 1. The active and reactive power flows in lines 15–17 and 34–35 (P_{15-17}, Q_{15-17} and P_{34-35}, Q_{34-35}) were used as additional real measurements in Scenario 2. Additional voltage measurements at buses 19, 20, and 21 (V_{19}, V_{20}, and V_{21}) were considered in Scenario 3 in line with [24].

Real measurements were modeled by adding small Gaussian uncertainty to the values obtained from load flow. The values obtained from load flow were used as mean values and 3% error around the mean was added. The load flow values with Gaussian uncertainty were used as input to both the ANN and to the state estimation function, as shown in Fig. 6.

Pseudo measurements were modeled following the methodology presented in Section IV. The number of mixture components used in the majority of loads was two.

Virtual measurements with very low error (10^{-8}) were used to model zero injection buses.

The ANN training, the error modeling, and the state estimation execution covered a whole year with half-hour steps (17 520 time steps). However, for clarity, results are presented after being sampled every 100 h (88 samples).

VI. Results and Discussion

The estimated values of the voltage magnitude and angle estimates for bus 6 (close to the substation) and bus 74 (remote from the substation) for Scenario 2 along with their true values and their $\pm 3\sigma$ confidence bounds for their estimates are shown in Figs. 8–11. It is noted that all estimates are within the confidence bounds with voltage angle estimates following the shape of the true value of the voltage angle more consistently.

The same values for bus 74 for Scenario 3 are shown in Figs. 12 and 13. It is evident that the additional voltage measurements have increased the matching between true and estimated voltage values and have made the confidence bounds narrower. In addition, it is observed that the additional voltage measurements have very small influence in the voltage angle estimates.

In terms of statistical evaluation, the average relative error (normalized with respect to the true value) was used. The average relative voltage magnitude and voltage angle errors for a specific bus (excluding the reference bus) are computed as follows:

$$e_V(\%) = \frac{100}{N} \sum_i \left| \frac{\hat{V}^i - V_t^i}{V_t^i} \right| \tag{9}$$

$$e_\delta(\%) = \frac{100}{N} \sum_i \left| \frac{\hat{\delta}^i - \delta_t^i}{\delta_t^i} \right| \tag{10}$$

where $\hat{V}^i$ is the voltage magnitude estimate, V_t^i is the true voltage magnitude, $\hat{\delta}^i$ is the voltage angle estimate, δ_t^i is the true voltage angle, i is the sampling step, and N is the number of sampling steps.

Figs. 14–17 show the relative voltage magnitude and voltage angle errors for bus 74 for Scenario 1 and Scenario 2. It can be seen that in Scenario 2, where the ANNs have three inputs, the accuracy of the state estimator is significantly improved in comparison with Scenario 1, where the ANNs have a single input. From the results, it can be concluded that increasing the number of input to the ANNs and/or increasing the number of voltage measurements improves the accuracy of state estimation, as expected.

In the scenarios presented, 54 sets of active and reactive power injection pseudo measurements were modeled with ANNs using one set (Scenario 1) or three sets (Scenario 2

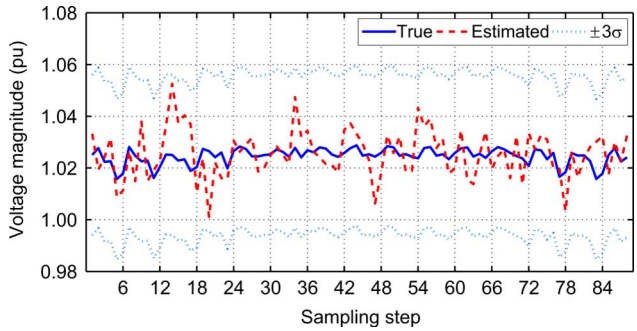

Fig. 8. Scenario 2—Bus 6 voltage magnitude.

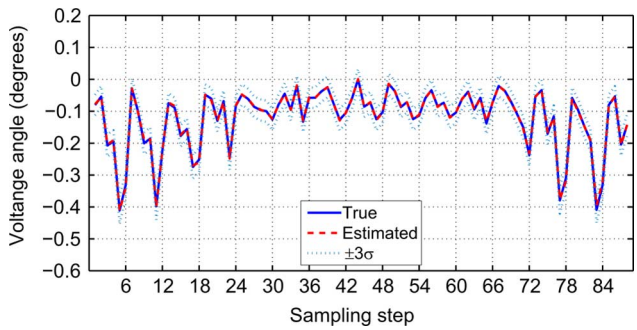

Fig. 9. Scenario 2—Bus 6 voltage angle.

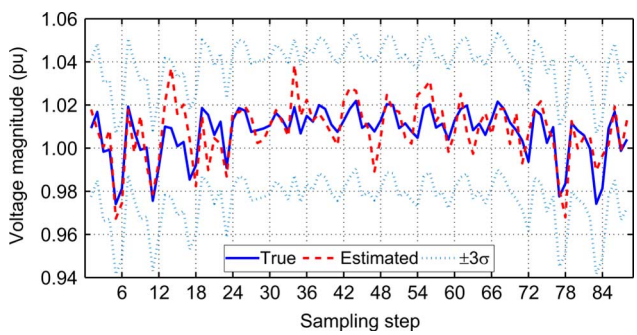

Fig. 10. Scenario 2—Bus 74 voltage magnitude.

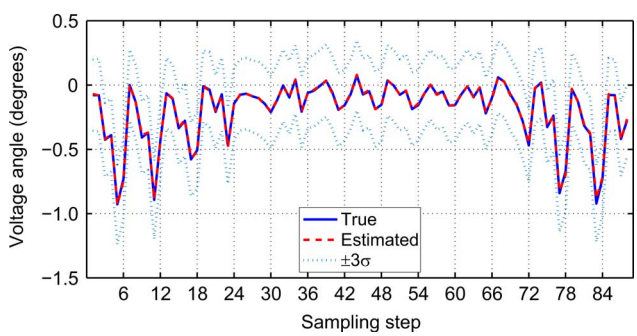

Fig. 11. Scenario 2—Bus 74 voltage angle.

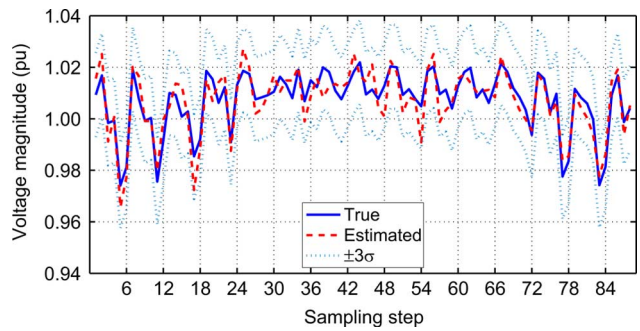

Fig. 12. Scenario 3—Bus 74 voltage magnitude.

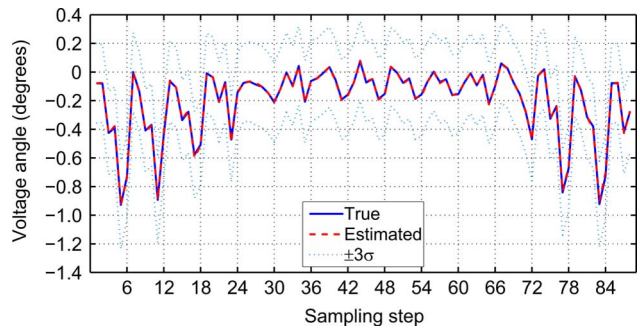

Fig. 13. Scenario 3—Bus 74 voltage angle.

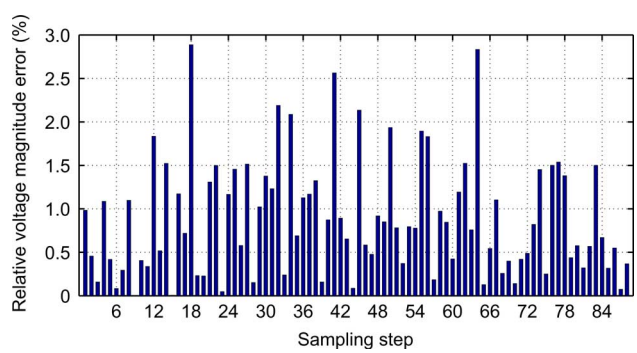

Fig. 14. Scenario 1—Bus 74 relative voltage magnitude error.

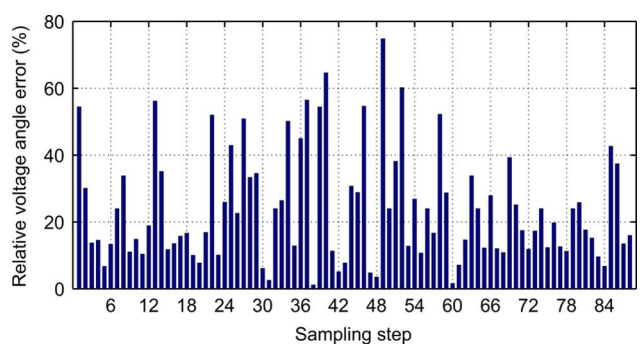

Fig. 15. Scenario 1—Bus 74 relative voltage angle error.

and 3) of real active and reactive power flow measurements. In effect, 54 sets of pseudo measurements were generated by monitoring 1% of the lines in Scenario 1 and 3% of the lines in Scenario 2 and 3 (the branch with buses 84 and 85 was ignored).

Table II presents the average relative voltage magnitude and voltage angle errors for bus 6 and bus 74 for all three scenarios and for both the ANN-based approach and using load profiles with 20% uncertainty as pseudo measurements. It is observed that although the average relative voltage magnitude error is similar (estimation of voltage magnitudes is directly affected by the available real voltage magnitude measurement in both cases), the proposed approach generates voltage angle estimates

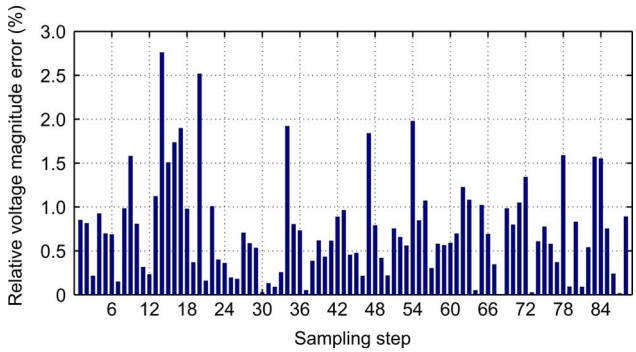

Fig. 16. Scenario 2—Bus 74 relative voltage magnitude error.

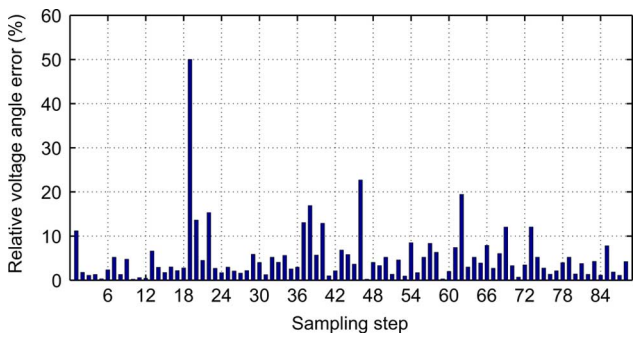

Fig. 17. Scenario 2—Bus 74 relative voltage angle error.

TABLE II
AVERAGE RELATIVE ERRORS

Scenario	State variable	Bus 6 (%)		Bus 74 (%)	
		ANN	Profile†	ANN	Profile†
1	Voltage magnitude	0.840	0.843	0.883	0.885
	Voltage angle	22.854	56.179	23.919	83.75
2	Voltage magnitude	0.711	0.799	0.741	0.847
	Voltage angle	4.404	40.310	5.180	64.08
3	Voltage magnitude	0.441	0.446	0.458	0.467
	Voltage angle	3.969	11.782	4.670	26.48

†20% error in load profile

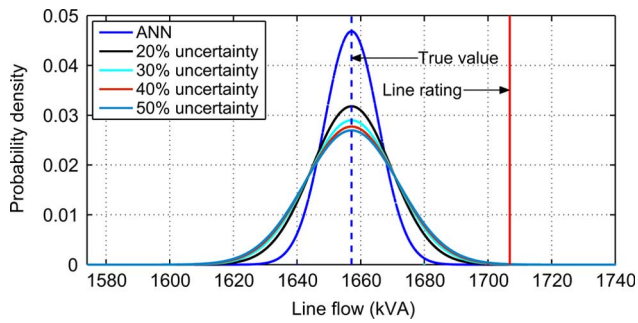

Fig. 18. Probability density of power flow estimate at line 2–4.

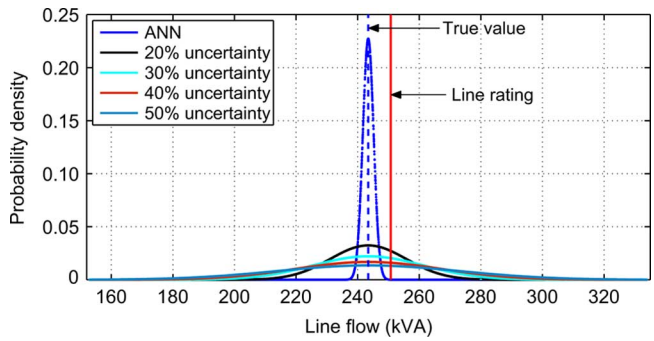

Fig. 19. Probability density of power flow estimate at line 10-11.

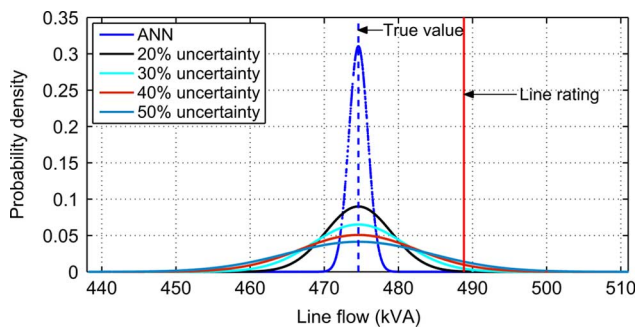

Fig. 20. Probability density of power flow estimate at line 72-74.

with significantly lower average relative error. Reducing the errors in the estimation of voltage angles is of particular importance as the accuracy of the computation of line power flows and currents is improved. As a result, equipment loading can be more effectively monitored.

In practice, voltage magnitude and angle estimates and estimation errors give limited insight to the distribution network operators (DNOs). DNOs are more interested in knowing the impact of estimates and estimation errors on the likelihood of a line being overloaded or a bus voltage magnitude being out of the statutory limits and their concern is whether this likelihood is captured by the state estimation function. As line power flows are functions of voltage magnitudes and voltage angle differences, any significant error in the voltage angle estimates will lead to poor line loading estimates. This is particularly important when lines operate close to their thermal limits.

In this context, the performance of the ANN-based approach is further evaluated through the accuracy of power flow estimates while lines are operating close to their thermal limits. To simulate this scenario, a snapshot of measurements on a typical winter day, when loads are high, is selected. The line power flows were estimated using the ANN-based pseudo measurement modeling approach. The true value of the line power flow was considered to be the mean of the estimate and its variance was computed using (6). To demonstrate the concept, it was assumed that the mean of the estimated power flows was around 97% of the line rating. Using the mean and variance, the probability densities of the estimated line power flows in all lines for Scenario 1 were computed.

The probability densities of power flow estimates in selected lines using the ANN-based approach are shown in Figs. 18–20. For comparison purposes, the probability densities of the estimated line power flows, computed using 20%, 30%, 40%, and 50% uncertainty in load pseudo measurements derived from average load profiles, are shown in the same figures. It is clear that the variation around the mean increases as the uncertainty in the load pseudo measurements increases. On the other hand, the variation is minimum in the case of the ANN-based approach.

TABLE III
PROBABILITY OF LINE OPERATING WITHIN THERMAL LIMITS $\Pr\left(\hat{S}_{flow} \leq S_{\max}\right)$

		Load uncertainty			
	ANN	20%	30%	40%	50%
Line 2-4	0.9999	0.9999	0.9998	0.9997	0.9996
Line 10-11	0.9999	0.7234	0.6572	0.6207	0.5978
Line 72-74	0.9999	0.9993	0.9900	0.9649	0.9301

This indicates that the ANN-based approach generates estimates that are close to the mean or the true value and, thus, offers high degree of confidence when the network operates close to its limits.

To verify this fact numerically, the probabilities of the lines operating within their thermal limits for the same cases were computed. The probabilities are shown in Table III. Line 2–4 is close to the main substation, where the only flow measurement is available, so the ANN-based approach only brings limited improvement on the probability. On the other hand, there is noticeable improvement in the probability of line 72–74 which is far from the main substation. Similarly, the power flow at line 10–11, which is immediately after the point where the system is split into two branches, sees significant improvement in the probability. In effect, by using the ANN-based approach, lines that are further away from the main substation can be operated closer to their ratings with greater confidence.

VII. COMPUTATIONAL REQUIREMENTS

The ANN training and testing, error modeling, and state estimation application were coded in MATLAB and run on a PC with Intel Xeon, 3.73-GHz processor with 4 GB of RAM. The computation time for training and testing each ANN was approximately 10 min, while the error association algorithm converged in 5 min. These times cover ANN training and testing using 17 520 sets of real power flow measurements and power injections, and error modeling using 17 520 errors. The maximum convergence time for the state estimation algorithm amongst all 88 samples was 0.7 s. ANN training, testing, and error modeling are offline tasks (not critical for real-time application) while DSSE is a near real-time function.

VIII. CONCLUSION

This paper presents an ANN-based approach to pseudo measurement modeling for DSSE. The proposed methodology uses load profiles and offline load flow analysis or historical data to train two ANNs, one for active and one for reactive power injections. The ANNs along with the associated error models are later used to model pseudo measurements in state estimation applications with a limited number of real power flow measurements. DSSE with the ANN-based approach for pseudo measurement modeling produces estimates of acceptable accuracy with a small number of real measurements.

The main advantage of the proposed approach is that the ANNs can effectively synchronize the average load profiles with the available real measurements and, by comparison with using average load profiles as pseudo measurements, generate pseudo measurements of better quality. As a result, with the DSSE function producing better quality estimates, network equipment can be operated close to its limits with greater confidence. Furthermore, the ANNs can easily be retrained to take into consideration annual load growth and system expansion. Likewise, the ANNs can be retrained when more real power flow measurements become available.

To demonstrate the concept of the proposed approach, the simulations in this paper assumed a fixed topology. However, distribution systems are subject to frequent topological changes due to switching or faults. To tackle this problem, ANNs can be trained in various network topologies, configurations, and contingencies so that pseudo measurements reflect a realistic state of the system. Alternatively, as described in [25], the critical network configurations can be stored in a model bank where each critical configuration will have a dedicated set of ANNs and an independent state estimation function. The proposed ANN-based methodology is generic in nature and can accommodate both options above.

The proposed methodology is most suited for MV networks where measurements are limited and network size is not very large. For larger networks, distributed state estimation and ANN training can be applied, after the network is split into several zones of manageable size.

The size and complexity of distribution systems call for new computational tools that can optimize the investment required for the introduction of AM in distribution systems. Being at the core of the DMS, a DSSE function generating acceptable accuracy estimates with the minimum number of real measurements will enable other DMS functions such as optimal power flow, contingency and security analysis, voltage regulation, voltage stability monitoring, fault level management, power quality assessment, to name just a few.

REFERENCES

[1] P. Djapic, C. Ramsay, D. Pudjianto, G. Strbac, J. Mutale, N. Jenkins, and R. Allan, "Taking an active approach," *IEEE Power Energy Mag.*, vol. 5, no. 4, pp. 68–77, Jul./Aug. 2007.
[2] I. Roytelman and S. M. Shahidehpour, "State estimation for electric power distribution systems in quasi real-time conditions," *IEEE Trans. Power Del.*, vol. 8, no. 4, pp. 2009–2015, Oct. 1993.
[3] M. E. Baran and A. W. Kelley, "State estimation for real-time monitoring of distribution systems," *IEEE Trans. Power Syst.*, vol. 9, no. 3, pp. 1601–1609, Aug. 1994.
[4] C. N. Lu, J. H. Teng, and W.-H. E. Liu, "Distribution system state estimation," *IEEE Trans. Power Syst.*, vol. 10, no. 1, pp. 229–240, Feb. 1995.
[5] W.-M. Lin and J.-H. Teng, "Distribution fast decoupled state estimation by measurement pairing," *Proc. Inst. Elect. Eng., Gen., Transm., Distrib.*, vol. 143, no. 1, pp. 43–48, Jan. 1996.
[6] A. Bernieri, G. Betta, C. Liguori, and A. Losi, "Neural networks and pseudo-measurements for real-time monitoring of distribution systems," *IEEE Trans. Instrum. Meas.*, vol. 45, no. 2, pp. 645–650, Apr. 1996.
[7] A. A. D. Silva, "A probabilistic associative memory and its application to signal processing in electrical power systems," *Eng. Appl. Artif. Intell.*, vol. 5, no. 4, pp. 309–318, Jul. 1992.
[8] V. Miranda, J. Pereira, and J. T. Saraiva, "Load allocation in DMS with a fuzzy state estimator," *IEEE Trans. Power Syst.*, vol. 15, no. 2, pp. 529–534, May 2000.
[9] A. K. Ghosh, D. L. Lubkeman, M. J. Downey, and R. H. Jones, "Distribution circuit state estimation using a probabilistic approach," *IEEE Trans. Power Syst.*, vol. 12, no. 1, pp. 45–51, Feb. 1997.
[10] E. Manitsas, R. Singh, B. C. Pal, and G. Strbac, "Modelling of pseudo-measurements for distribution system state estimation," in *Proc. CIRED Seminar 2008: SmartGrids for Distribution*, Jun. 2008.

[11] D. Gerbec, S. Gasperic, I. Smon, and F. Gubina, "Allocation of the load profiles to consumers using probabilistic neural networks," *IEEE Trans. Power Syst.*, vol. 20, no. 2, pp. 548–555, May 2005.
[12] A. P. Alves da Silva, V. H. Quintana, and G. K. H. Pang, "Solving data acquisition and processing problems in power systems using a pattern analysis approach," *Proc. Inst. Elect. Eng., Gen., Transm., Distrib. C*, vol. 138, no. 4, pp. 365–376, Jul. 1991.
[13] R. Singh, B. C. Pal, and R. A. Jabr, "Distribution system state estimation through Gaussian mixture model of the load as pseudo-measurement," *IET Gen., Transm., Distrib.*, vol. 4, no. 1, p. 50, Jan. 2010.
[14] R. Singh, B. C. Pal, and R. A. Jabr, "Choice of estimator for distribution system state estimation," *IET Gen., Transm., Distrib.*, vol. 3, no. 7, pp. 666–678, Jul. 2009.
[15] A. Abur and A. G. Expósito, *Power System State Estimation: Theory and Implementation*. New York: Marcel Dekker, 2004.
[16] E. Caro, A. J. Conejo, and R. Minguez, "Power system state estimation considering measurement dependencies," *IEEE Trans. Power Syst.*, vol. 24, no. 4, pp. 1875–1885, Nov. 2009.
[17] F. L. Lewis, *Optimal Estimation*. New York: Wiley, 1986.
[18] H. S. Hippert, C. E. Pedreira, and R. C. Souza, "Neural networks for short-term load forecasting: A review and evaluation," *IEEE Trans. Power Syst.*, vol. 16, no. 1, pp. 44–55, Feb. 2001.
[19] S. S. Haykin, *Neural Networks: A Comprehensive Foundation*. Englewood Cliffs, NJ: Prentice-Hall, 1999.
[20] M. F. Møller, "A scaled conjugate gradient algorithm for fast supervised learning," *Neural Netw.*, vol. 6, no. 4, pp. 525–533, 1993.
[21] Matlab Neural Network Toolbox™ 6, User's Guide. [Online]. Available: http://www.mathworks.com.
[22] R. Singh, B. C. Pal, and R. A. Jabr, "Statistical representation of distribution system loads using Gaussian mixture model," *IEEE Trans. Power Syst.*, vol. 25, no. 1, pp. 29–37, Feb. 2010.
[23] United Kingdom Generic Distribution Network (UKGDS). [Online]. Available: http://monaco.eee.strath.ac.uk/ukgds/.
[24] R. Singh, B. C. Pal, and R. B. Vinter, "Measurement placement in distribution system state estimation," *IEEE Trans. Power Syst.*, vol. 24, no. 2, pp. 668–675, May 2009.
[25] R. Singh, E. Manitsas, B. C. Pal, and G. Strbac, "A recursive Bayesian approach for identification of network configuration changes in distribution system state estimation," *IEEE Trans. Power Syst.*, vol. 25, no. 3, pp. 1329–1336, Aug. 2010.

Efthymios Manitsas (M'06) received the Dipl.-Eng. degree in electrical and computer engineering from Aristotle University of Thessaloniki, Thessaloniki, Greece, and the M.Sc. degree in sustainable electricity systems from the University of Manchester Institute of Science and Technology (UMIST), Manchester, U.K., in 2003 and 2004, respectively. He is currently pursuing the Ph.D. degree at Imperial College London, London, U.K.

His current research interests include active distribution networks and distribution system state estimation.

Ravindra Singh (S'07–M'09) is a postdoctoral fellow in the Department of Electrical and Electronic Engineering, Imperial College London, London, U.K. His current research interests include distribution system state estimation.

Bikash C. Pal (M'00–SM'02) is a Reader in the Department of Electrical and Electronic Engineering, Imperial College London, London, U.K. His current research interests include state estimation, power system dynamics, and flexible ac transmission system controllers.

Goran Strbac (M'95) is a Professor in the Department of Electrical and Electronic Engineering, Imperial College London, London, U.K. His current research interests include distribution system state estimation, electricity generation, transmission and distribution operation, planning and pricing, and integration of renewable and distributed generation in electricity systems.